

## Phason-strain-field influences on low-temperature specific heat in icosahedral quasicrystals Al-Li-Cu and Al-Fe-Cu

K. Wang and P. Garoche

*Laboratoire de physique des solides, Centre National de la Recherche Scientifique, Université Paris-Sud, 91405 Orsay, France*

(Received 22 July 1996)

We investigated the phason-strain-field influences on electronic and vibrational properties of two icosahedral quasicrystals, Al-Li-Cu and Al-Fe-Cu. For that purpose we performed low-temperature specific-heat measurements on samples before and after annealing treatments that allowed strong phason-strain elimination. The electronic specific heat for the two systems is found to be scarcely sensitive to the annealing treatments, while the vibrational specific heat displays a different behavior: it remains unchanged in Al-Li-Cu, but is strongly reduced in Al-Fe-Cu after annealing. We interpret this to arise from the correlation between the symmetry of the phason-strain field and the electronic and vibrational properties. [S0163-1829(97)02201-7]

### I. INTRODUCTION

Phason strains describe particular structural disorders, or structure fluctuations, in quasicrystals (QC). The possibility of the phason-strain existence in QC's was evoked soon after the discovery of the quasicrystalline Al-Mn phase,<sup>1</sup> and was later formulated based on a six-dimension space description.<sup>2</sup> Phason excitations were also described in an order-parameter space.<sup>3</sup> Structure fluctuations in icosahedral QC's can be characterized by three bulk translation modes and three relative phase-shift modes associated with internal atomic position rearrangements. These modes are, respectively, described in the parallel and the perpendicular spaces. Spatially uniform displacements in both spaces leave the system free energy invariant. Spatially varying displacements in the parallel space are described by the phonon strains, while that in the perpendicular space by phason strains. In a continuous model, these displacements are described by hydrodynamic modes.<sup>4,5</sup>

According to the group theory treatments, phason-strain field in an icosahedral QC system can be classified according to their symmetry properties. Two types of phason-strain fields can be deduced, that transform, respectively, under  $\Gamma_4$  and  $\Gamma_5$ , which are the four- and five-dimension representations of the icosahedral group.<sup>4,6,7</sup> From the structural point of view, these two phason-strain fields break the icosahedral symmetry and lead to structures belonging to subgroups of the icosahedral group I. For example, a phason-strain field transforming under the  $\Gamma_5$  representation, here after noted  $\Gamma_5$  field, can lead to  $D_5$  (pentagonal) or  $D_3$  (rhombohedral) structures, and a phason-strain field transforming under the  $\Gamma_4$  representation, here after noted  $\Gamma_4$  field, can lead to  $T$  (tetrahedral) structures.<sup>6,7</sup>

Phason strains are considered to play an important role in the atomic structural properties of QC's. For example, they can be related to special structure distortions<sup>8</sup> and structure imperfections, such as dislocations.<sup>9</sup> However, what are the physical implications of the phason-strain-field presence in QC's, since physical properties of condensed matters are related to their corresponding atomic structures? In a more limited way, a phason-strain field in QC's causes distortions

in the reciprocal lattice,<sup>8</sup> how will such distortions affect the lattice vibrational properties? Besides, reciprocal-lattice distortions modify the electronic structure, will the Hume-Rothery stabilization condition<sup>10</sup> be consequently altered? In this paper we discuss the situation of two families of icosahedral QC's, in relation to our low-temperature specific-heat measurements on the Al-Li-Cu and Al-Fe-Cu QC phases. Parts of this work have been published elsewhere in condensed preliminary forms.<sup>11</sup>

### II. PHASON-STRAIN FIELDS IN Al-Li-Cu AND Al-Fe-Cu

The Al-Li-Cu and Al-Fe-Cu icosahedral phases differ from each other in many ways. In the cut-and-projection description, the Al-Li-Cu QC phase belongs to a six-dimension primitif ( $P$ ) cubic lattice, while the Al-Fe-Cu QC phase belongs to a face-centered ( $F$ ) cubic lattice. As far as the growth mode is concerned, Al-Li-Cu grows preferentially along twofold axes, and Al-Fe-Cu along fivefold axes. Furthermore, the atomic structures of these two phases are considered to be different: Al-Li-Cu is characterized by Bergman clusters, while Al-Fe-Cu by Mackay clusters. The as-cast Al-Li-Cu samples, although obtained by slow cooling, contain considerable disorder.<sup>12</sup> On the contrary, Al-Fe-Cu sample quality can easily be improved after a relatively short annealing time.<sup>13</sup>

The as-cast Al-Li-Cu QC samples display deviations from the icosahedral symmetry.<sup>14</sup> Their diffraction spots are observed to be shifting along twofold axes.<sup>15</sup> Mai *et al.*<sup>16</sup> and Li *et al.*<sup>17</sup> have shown that the diffraction spot shifts in as-cast Al-Li-Cu samples are characterized by the presence of a linear phason-strain field. Using a tensor that acts on the atomic positions in the physical space to describe the field, this tensor is characterized by the following matrix  $M$ :

$$M = \begin{bmatrix} -1 & 0 & 0 \\ 0 & 0 & -1 \\ 0 & 1 & 0 \end{bmatrix}.$$

This matrix can be compared with the one ( $M_T$ ) obtained by Ishii,<sup>6</sup> that describes a phason-strain-field invariant under the  $\Gamma_4$  symmetry operations:

$$M_T = \alpha_1 \begin{bmatrix} 1 & 0 & 0 \\ 0 & 1 & 0 \\ 0 & 0 & 1 \end{bmatrix},$$

where  $\alpha_1$  is a constant describing the field magnitude. It is straightforward to check that these two matrices are equivalent, and that the difference between them is simply due to the choice of the orthonormal set of six-dimension vectors.

Furthermore, the phason-strain-field symmetry in the Al-Li-Cu QC phase can also be analyzed in relation to the symmetry properties of its approximant phase. The spot shifts along the twofold icosahedral directions for Al-Li-Cu are associated with the structure transformation between the QC phase and the  $R$  phase, which belongs to the  $T$  point group<sup>18</sup> and is considered as an approximant phase, in the sense that a rational number is an approximant to an irrational one. Such a structure transformation, from icosahedral to tetrahedral symmetry, can actually be induced by developing a  $\Gamma_4$  phason-strain field in the icosahedral phase.<sup>6,7</sup> These analyses show that the phason-strain field in the as-cast Al-Li-Cu can essentially be described by a field invariant under the  $\Gamma_4$  symmetry operations.

For the Al-Fe-Cu case, although there is no direct characterization of the phason-strain field, it has been observed that the phason strains in this system show transformation trends towards either pentagonal or rhombohedral phases.<sup>19</sup> Actually, both of these two phases are approximant phases of the icosahedral one, and can be related to the later through phason-strain fields that are invariant under the  $\Gamma_5$  symmetry operations. As an example, a  $\Gamma_5$  field can induce structure modulations along one of the fivefold axes and leads to  $D_5$  subgroup structures, that is a pentagonal phase.<sup>6,7</sup>

Further, it has been observed by high-resolution electron microscopy that the structure transformation from icosahedral to pentagonal symmetries in Al-Fe-Cu can be described by the phason-strain field effect which is associated to the following matrix  $M_{D_5}$  ( $\alpha_2$  being a constant and describing the field magnitude):<sup>20</sup>

$$M_{D_5} = \alpha_2 \begin{bmatrix} 1 & 1/\tau & 0 \\ -\tau & -1 & 0 \\ 0 & 0 & 0 \end{bmatrix}.$$

According to Ref. 6, this matrix describes exactly a phason-strain-field invariant under the  $\Gamma_5$  symmetry operations. All this suggests that the phason-strain field in Al-Fe-Cu has a  $\Gamma_5$  character.

### III. PHASON-STRAIN FIELDS, ELECTRONIC STRUCTURE, AND ELASTICITY

#### A. Electronic structure

It is now generally agreed that the stabilization of the icosahedral structure has an electronic origin, which can be explained within a Hume-Rothery-like framework. The wave vectors in the reciprocal space display a large multiplicity, due to the high symmetry degree of the icosahedral lattice. The diffusion potentials defined upon such vectors, lead to a highly spherical pseudo-Brillouin zone (PBZ) near the Fermi surface, upon which the electronic states are perturbed al-

most everywhere. A pseudogap is then opened in the electronic density of states (DOS) at the Fermi level. The electronic cohesive energy is thus increased.<sup>10</sup>

A phason-strain field in QC's causes distortions to the reciprocal lattice by shifting the wave vectors, this will deform the PBZ which is built upon the wave vectors close to the Fermi sphere. In other words, a phason-strain field modifies the structure relation between the Fermi surface and the PBZ by making the later less spherical, since any deviation from the perfect icosahedral lattice reduces the point symmetry.

For given chemical compositions, the icosahedral structure remains stable down to room temperature. This implies that it can be considered as the fundamental state. It is therefore not ambiguous to assume that, by deforming the PBZ, a phason-strain field affects the pseudogap at the Fermi level, and that consequently it costs cohesive energy. The observation that annealing treatments improve the structure quality by eliminating the phason strains supports this proposition.

The quasiperiodicity implies another specificity for the QC's. At variance with crystals, the Fourier transform of a quasiperiodic lattice is characterized by a dense set of Bragg vectors. This situation has an original consequence on the electronic structure of icosahedral QC's: the Fermi surface displays a hierarchy of gaps with different width. All the gaps close to the Fermi surface contribute to the electronic cohesive energy, but they undergo different shifts under a phason-strain field. As we will see below, this has some particular consequences on the relationship between the electronic structure and the phason-strain field.

#### B. Elasticity

The elastic free energy is the product of the strain by the stress. In Hook's approximation, the stress is proportional to the strain, so the elastic free energy is expressed by a quadratic form of the elastic deformations, and it has the following general form for QC's:<sup>5</sup>

$$F_{el} = \frac{1}{2} \int d^d (K_{ijkl}^{uu} \nabla_i u_j \nabla_k u_l + K_{ijkl}^{ww} \nabla_i w_j \nabla_k w_l + K_{ijkl}^{uw} \nabla_i u_j \nabla_k w_l), \quad (1)$$

where  $\{K\}$  is elastic tensor, while  $\nabla_i u_j$  and  $\nabla_i w_j$  describe, respectively, phonon and phason deformations.

The six-dimension representation of the icosahedral group  $\Delta$  can be decomposed into two irreducible representations, respectively, in the physical and the perpendicular spaces:<sup>4</sup>

$$\Delta = \Gamma_3 + \Gamma'_3. \quad (2)$$

The gradient operator  $\nabla$  transforms as  $\Gamma_3$ . Thus, in Eq. (1), the deformations  $\nabla_i u_j$  and  $\nabla_i w_j$  are, respectively, described by the representations  $\Gamma_3 \times \Gamma_3$  and  $\Gamma_3 \times \Gamma'_3$ . These two representations can in turn be decomposed as follows:

$$\Gamma_3 \times \Gamma_3 = \Gamma_1 + \Gamma_3 + \Gamma_5, \quad (3)$$

$$\Gamma_3 \times \Gamma'_3 = \Gamma_4 + \Gamma_5. \quad (4)$$

The number of second-order invariants in Eq. (1) can be obtained from these two decompositions. In the decomposi-

tion of Eq. (3),  $\Gamma_3$  represents a rotation, and has no continuous symmetry associated to it;<sup>4</sup>  $\Gamma_1$  and  $\Gamma_5$  describe phonon modes, they represent, respectively, the dilatation and the shear.  $\Gamma_4$  and  $\Gamma_5$  in Eq. (4) represent the two phason-strain fields. Since the  $\Gamma_3$  phason-strain field and the  $\Gamma_5$  phonon field both belong to the same representation, there can be a coupling effect between these two fields. Thus the lattice vibrational properties in icosahedral QC's can be affected by the  $\Gamma_5$  phason-strain-field presence. As far as the  $\Gamma_4$  phason-strain field is concerned, no coupling is possible between this field and any of the two phonon fields, as neither of these two phonon fields transform under the  $\Gamma_4$  representation.

#### IV. EXPERIMENTAL

In order to study the phason-strain influence on the electronic and vibrational properties of the Al-Li-Cu and Al-Fe-Cu QC phases, we have investigated the low-temperature specific-heat evolution on phason-strained and phason-eliminated QC samples of these two phases.

The low-temperature specific-heat measurement enables experimental investigations of the phason strain influence on the electronic structure and the elastic behavior. On one hand, the electronic specific heat for metals is directly proportional to the electronic density of states (DOS) at the Fermi level. The DOS evolution is therefore susceptible to reveal eventual electronic-structure alterations due to the phason-strain-field presence.

On the other hand, the specific-heat vibrational term is determined by thermodynamic properties, which are intimately related to the elastic properties of solids. At low temperature, long-wavelength vibrational modes are excited, and the later are related to macroscopic elastic constants in a continuum model approximation. This vibrational term therefore enables the investigation of phason-strain-field effects on the quasilattice long-wavelength vibrational (elastic) properties.

##### A. Sample preparations

The Al-Li-Cu samples, of composition  $\text{Al}_6\text{Li}_3\text{Cu}$ , are first elaborated using the method described by Dubost *et al.*<sup>21</sup> They are obtained in the form of triacontahedral dendrites, embedded in eutectic phases (mainly  $\alpha$ -Al and  $T_1$ - $\text{Al}_2\text{LiCu}$ ). Then, in order to eliminate these eutectic phases, the samples are remelted and once more solidified through slow cooling, taking advantage of the fact that the QC phase floats on its eutectic liquid. The samples obtained are single phased according to the x-ray-diffraction experiments. The final stage consists of annealing the samples at 575 °C during several days. In the last two stages, the samples are maintained under an inert gas pressure (about 50 bars at 575 °C) to prevent lithium evaporation. The structure evolution is characterized by transmission electron microscopy investigation. Two samples, obtained, respectively, by slow cooling and by annealing (10 days) are investigated, in comparison with our previous observations on the as-cast samples.<sup>22</sup>

Electron-diffraction patterns show that, through spot displacements along twofold directions, the diffraction-spot shifts observed for the as-cast samples, as well as for the slow-cooled ones, are strongly reduced on the 10 days annealed sample. The spot positions for the annealed sample

approach the ones expected for a perfect icosahedral structure. This indicates that the samples before and after annealing differ from each other by the magnitude of the phason-strain field, the phason-strain field present in the samples before annealing are strongly eliminated by the thermal treatments (more details are given elsewhere<sup>23</sup>).

The Al-Fe-Cu samples, of nominal composition  $\text{Al}_{62}\text{Cu}_{25.5}\text{Fe}_{12.5}$ , are elaborated at the CECM/CNRS in Vitry (France). They are obtained by planar flow casting and then submitted to various thermal treatments. This composition produces different structural states according to the thermal treatment: an annealing at 600 °C leads to a single-phased but phason-strained QC structure; whereas a further annealing up to 812 °C eliminates the phason strain.

Two samples, obtained, respectively, after the 600 °C and the 812 °C annealing, are studied. High-resolution x-ray-diffraction experiments show that both of them are single phased. For the 600 °C annealed sample, the x-ray Bragg peaks are shifted and broadened. This sample can thus be considered to contain essentially frozen-in phason strains,<sup>13</sup> though powder-diffraction investigation does not allow us to characterize directly the phason-strain field symmetry. For the 812 °C annealed sample, the phason strains are eliminated. The x-ray-diffraction peak width is of the order of the instrumental resolution ( $\Delta q \sim 10^{-3} \text{ \AA}^{-1}$ ), and the peak positions are almost those of an ideal icosahedral lattice. This sample remains stable through out the whole temperature range, from 812 °C down to room temperature.<sup>13</sup>

##### B. Specific-heat measurements

The low-temperature heat capacity is measured using an ac calorimetric method. For the Al-Li-Cu samples, the experiments are performed at a working frequency of about 1 Hz and in between a temperature range of 1 to 6 K. For the Al-Fe-Cu samples they are performed at frequencies from 2 to 6 Hz and in between a temperature range of 1 to 3 K. The sample masses are about 10 mg for Al-Li-Cu and about 1.5 mg for Al-Fe-Cu. The thermal oscillation amplitude was about 0.1 K. The samples are glued on a sample holder (thin sapphire slabs of  $2.5 \times 6 \times 0.2$  mm, on which a heater, a thermometer, and thermal links are deposited) using the M-Bond adhesive of Measurements Group Inc. Taking into account the weak heat capacity of these samples (below 20 nJ/K at 1 K for Al-Fe-Cu), the heat capacity of the sample holders with glue are measured in separate runs and their contribution (several nJ/K at 1 K) is subtracted from the total heat capacity. The molar specific heat  $C$  of the Al-Li-Cu and Al-Fe-Cu samples, before and after annealing, is presented in Figs. 1(a) and 1(b) as a function of the temperature.

The plots in the insets show that in the measuring temperature ranges, the specific heat for all the samples can be described within 1% by the classical law  $C = \gamma T + \beta T^3$ . This enables the separation between the electronic contribution  $\gamma T$  and the vibrational one  $\beta T^3$ . We notice that the  $T^3$  temperature dependence of the vibrational term suggests a Debye model description for all the samples. The  $\gamma$  and  $\beta$  values for these two alloys are obtained by a best fit of the data, and listed in Table I. The error on the absolute value is estimated to be within 2% for  $\gamma$  and 5% for  $\beta$ , taking into account all the experimental uncertainties.

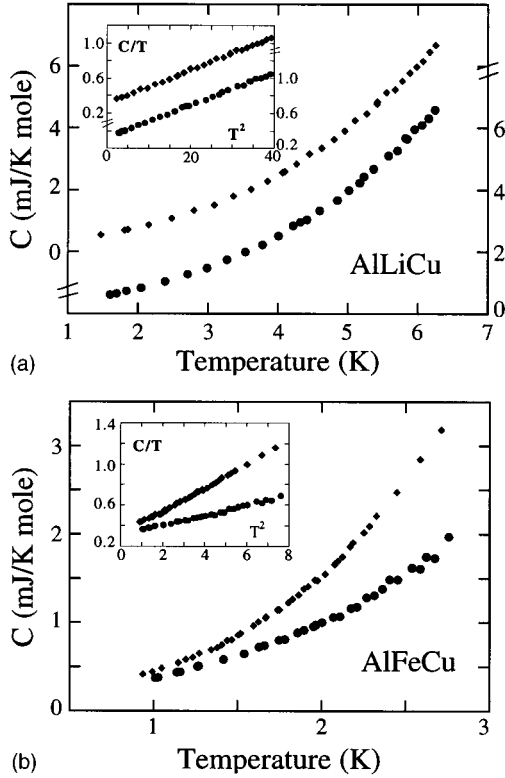


FIG. 1. The molar specific heat  $C$  of the icosahedral Al-Li-Cu (a) and Al-Fe-Cu (b) samples, before ( $\blacklozenge$ ) and after ( $\bullet$ ) the annealing treatments that allowed phason-strain-field eliminations. In the insets are presented the data replotted in a  $C/T$  versus  $T^2$  diagram.

## V. DISCUSSION

According to Table I, the electronic contribution remains the same ( $\gamma=0.33$  mJ/K<sup>2</sup> mole) for Al-Li-Cu before and after the annealing treatment, while for Al-Fe-Cu, the  $\gamma$  value only changes slightly from 0.33 to 0.30 mJ/K<sup>2</sup> mole after the 812 °C annealing. These results are close to the ones obtained in other observations.<sup>24–26</sup> All of these values actually represent about one third of that predicted by a free-electron model.

It is well known that the  $\gamma$  value is proportional to the electronic DOS at the Fermi level  $n(E_F)$  according to the classical relation:<sup>27</sup>

$$\gamma = \frac{1 + \lambda}{3} \pi^2 k_B^2 n(E_F), \quad (5)$$

TABLE I. Coefficients of the low-temperature specific heat,  $\gamma$  (electronic) and  $\beta$  (vibrational), obtained for the icosahedral Al-Li-Cu and Al-Fe-Cu samples before and after annealing treatments.

	$\gamma$ (mJ/K <sup>2</sup> mole)	$\beta$ (mJ/K <sup>4</sup> mole)
Al-Li-Cu: before annealing	0.33	0.019
after annealing	0.33	0.019
Al-Fe-Cu: before annealing	0.33	0.115
after annealing	0.30	0.045
Error	$\pm 2\%$	$\pm 5\%$

where  $\lambda$  is a constant related to the ratio between the electron thermal effective mass and the free electron mass,  $k_B$  is the Boltzmann constant. This indicates that the electronic DOS at the Fermi level is scarcely sensitive to the phason-strain elimination in these two systems.

The  $T=0$  Debye temperature,  $\theta_{D0}$ , can be calculated from the  $\beta$  values using the following relation:<sup>27</sup>

$$\beta = \frac{12\pi^4}{5} \frac{Nk_B}{\theta_{D0}}, \quad (6)$$

where  $N$  is the Avogadro number. For both of the Al-Li-Cu samples we obtain  $\theta_{D0}=465 \pm 5$  K, which is close to the values given by Wagner *et al.*<sup>24</sup> This value can be compared to our previous observation on as-cast Al-Li-Cu samples,<sup>22</sup> where the  $\theta_{D0}$  value for the whole sample was estimated as  $450 \pm 10$  K. However, if we take into account the presence of about 15 to 20% of foreign phases (mainly  $\alpha$ -Al and  $T_1$ -Al<sub>2</sub>LiCu) in these samples, the  $\theta_{D0}$  value for the QC phase in the as-cast samples is about  $460 \pm 10$  K. This indicates that the vibrational contribution, as well as the Debye temperature at low temperature remain nearly unchanged from as-cast sample to annealed one passing by slow-cooled one, while the phason-strain field is strongly eliminated.

The situation for the Al-Fe-Cu samples is totally different, the  $\beta$  value changes from 0.115 mJ/K<sup>4</sup> mole for the phason-strained sample to 0.045 mJ/K<sup>4</sup> mole for the 812 °C annealed one. This implies that the Debye temperature  $\theta_{D0}$  increases from  $273 \pm 5$  K to  $350 \pm 5$  K after the 812 °C annealing treatment. We can notice that the  $\theta_{D0}$  value for the annealed sample is somewhat lower than the one obtained by Biggs, Li, and Poon,<sup>25</sup> but is in agreement with the value given by Klein *et al.*<sup>26</sup>

### A. Electronic

The electronic DOS at the Fermi level remains nearly unchanged in all the samples before and after the annealing treatments, which allowed phason-strain-field elimination. This indicates that the pseudogap at the Fermi level is scarcely sensitive to the phason-strain fields of these two systems. The Fermi level remains in the pseudogap, which suggests that the PBZ deformations due to the phason-strain fields have no significant effects on the neighborhood relation between the Fermi sphere and the PBZ.

In order to explain this observation, we notice two aspects in the Hume-Rothery stabilization mechanism for QC's. The first one concerns the electronic structure: all the vectors constructing the PBZ do not contribute by the same magnitude to the total electron energy. A Bragg plane corresponding to a potential  $V_{\mathbf{K}}$ , leads to a gap of  $2V_{\mathbf{K}}$  width in the electron dispersion relation, thus the gap width varies with the vectors. The second aspect is specific to the QC structure: in the presence of a phason-strain field, the reciprocal vector shift  $\Delta K$  varies according to the corresponding perpendicular vectors  $K_{\perp}$  in the perpendicular reciprocal space. The vectors correspond to larger  $K_{\perp}$  undergo stronger shifts, it is those vectors that correspond to weaker  $V_{\mathbf{K}}$  values in the (physical) reciprocal space.

Now let us consider the Al-Li-Cu and Al-Fe-Cu QC phases. The Hume-Rothery stabilization implies for the PBZ vectors  $K_{\text{PBZ}}$  the following condition:<sup>10</sup>

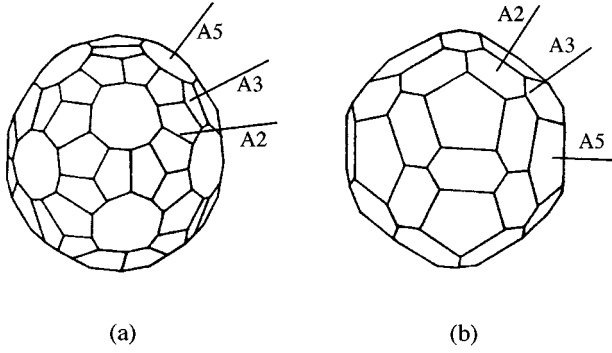


FIG. 2. The pseudo-Brillouin zones (PBZ) for Al-Li-Cu (a tricosahedron truncated by a dodecahedron) (a) and Al-Fe-Cu (a dodecahedron truncated by a triacontahedron) (b) icosahedral phases. A2, A3, and A5 indicate, respectively, the two-, three-, and fivefold symmetry axes.

$$K_{\text{PBZ}} \approx 2k_F,$$

where  $k_F$  is the Fermi vector. Taking a free-electron model, we estimate for the Al-Li-Cu QC phase  $k_F \approx 1.9 \text{ \AA}^{-1}$  and for the Al-Fe-Cu QC phase  $k_F \approx 1.56 \text{ \AA}^{-1}$ . We can construct for the Al-Li-Cu QC phase a PBZ formed by a tricosahedron which is built upon 60 26–41 vectors, and is truncated by a dodecahedron built upon 12 28–44 vectors [Fig. 2(a)]. In the same way, we can construct for the Al-Fe-Cu QC phase a PBZ formed by a dodecahedron, built upon 12 18–29 vectors, and truncated by a triacontahedron built upon 30 20–32 vectors [Fig. 2(b)]. Here we use the Cahn-Shechtman-Gratias  $N$ - $M$  notation,<sup>28</sup> where the magnitude of a vector  $N$ - $M$  in the physical (parallel) space is given by

$$K^{N,M} = \frac{2\pi}{A_6} \sqrt{\frac{N+M\pi}{2(2+\pi)}}, \quad (7)$$

while the magnitude of its perpendicular vector is given by

$$K_{\perp}^{N,M} = \frac{2\pi}{A_6} \sqrt{\frac{N\tau - M}{2(2+\pi)}}, \quad (8)$$

where  $A_6$  is the six-dimension lattice parameter,  $\tau$  is the golden number.  $N$  and  $M$  are both integers. The 28–44 and 20–32 vector sets are characterized by larger perpendicular vectors  $K_{\perp}$  than the 26–41 and 18–29 ones:

$$\frac{K_{\perp}^{20,32}}{K_{\perp}^{18,29}} \approx 1.7, \quad \frac{K_{\perp}^{28,44}}{K_{\perp}^{26,41}} \approx 1.1.$$

Therefore they correspond to weaker diffraction intensity, and thus to weaker  $V_{\mathbf{K}}$ , that lead to narrower gaps than the 26–41 and 18–29 sets. Furthermore, the magnitudes of their perpendicular vectors  $K_{\perp}$  being larger, the 28–44 and 20–32 vectors undergo stronger shifts under a given phason-strain field.

In the Hume-Rothery stabilization mechanism, the electron cohesive energy is more sensitive to the positions of narrower gaps than that of larger ones at the Fermi level. To illustrate this mechanism in a schematic manner, let us consider the opening of a  $2V_{\mathbf{K}}$  width gap that perturbs the electronic states in an interval  $\Delta K$  of the reciprocal space [see Fig. 3(a)]:

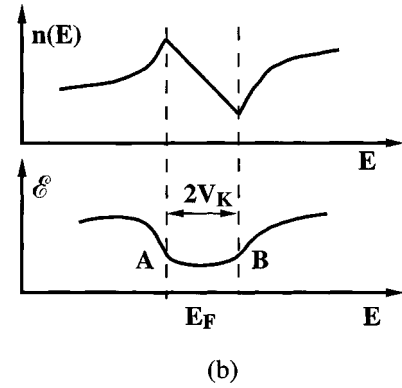
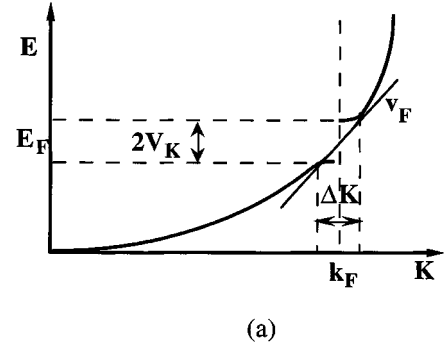


FIG. 3. Schematic representation of the opening of a gap of  $2V_{\mathbf{K}}$  in width at the Fermi level (a), leading to a minimum in the electron total energy  $\mathcal{E}$  (b).

$$\Delta K = \frac{2V_{\mathbf{K}}}{v_F}, \quad (9)$$

where  $v_F$  is the unperturbed Fermi velocity,  $v_F = 2E_F/k_F$ . The  $2V_{\mathbf{K}}$  gap induces two kinks in the electronic DOS  $n(E)$ , and a minimum in the electronic total energy  $\mathcal{E} = \int n(E)dE$  [Fig. 3(b)]. The width of this minimum is determined by the gap width  $2V_{\mathbf{K}}$ , which is related to  $\Delta K$  through Eq. (9). The system has the maximal cohesive energy gain if the gap is situated at the Fermi level. So, if the vector shift is weak compared to  $\Delta K$ , which measures the gap width in the reciprocal space, the Fermi level remains within the total-energy minimum, and the potential  $V_{\mathbf{K}}$ 's contribution to the electron cohesive energy will not be significantly modified. But on the contrary, if the shift is stronger than  $\Delta K$ , the Fermi level goes out of the minimum, and the contribution of the corresponding  $V_{\mathbf{K}}$  to the cohesive energy will be strongly decreased. Therefore, a phason-strain field affects the electron cohesive energy first through the shift of weaker  $V_{\mathbf{K}}$  vectors near the Fermi surface, which correspond to stronger  $K_{\perp}$  and narrower gaps. For strong  $V_{\mathbf{K}}$  vectors, the phason-strain-field-induced shifts are weak due to the weaker magnitude of the perpendicular vector  $K_{\perp}$ , and, moreover, the corresponding gaps are large, therefore less sensitive to small shifts.

In order to cost less electron cohesive energy, a phason-strain field should thus shift as little as possible the wave vectors corresponding to stronger  $K_{\perp}$  near the Fermi surface. This consideration enables us to discuss the relationship be-

tween the phason-strain field and the electronic structure, by simply using symmetry arguments, without going into details of atomic and band structures. In the following, we apply this simple model to the Al-Li-Cu and Al-Fe-Cu case.

Let us consider the two phason-strain field matrices  $M_T$  and  $M_{D5}$ , describing, respectively, a  $\Gamma_4$  and a  $\Gamma_5$  phason-strain field (see Sec. II). The shift  $\Delta\mathbf{K}$  of the vectors 20–32 and 28–44 under these two fields can be easily calculated using Eq. (10):<sup>8</sup>

$$\Delta\mathbf{K} = \mathbf{M} \cdot \mathbf{K}_\perp. \quad (10)$$

The 12 vectors of the 28–44 set, parallel to the fivefold axes and generating the dodecahedron of the Al-Li-Cu PBZ are indexed by  $(2/2, 2/4, 0/0)$ ,  $(\sqrt{2}/\sqrt{2}, 2/4, 0/0)$ ,  $\dots$ , and their perpendicular vectors  $\mathbf{K}_\perp$  by  $(2/2, 4/2, 0/0)$ ,  $(\sqrt{2}/2, 4/2, 0/0)$ ,  $\dots$ . It is straightforward, using Eq. (10), to check that these vectors undergo a  $\Delta\mathbf{K}$  shift that is perpendicular to themselves under  $M_T$ , while the  $M_{D5}$  field leads to stronger vector magnitude variations with a component along the  $\mathbf{K}$  directions [see Fig. 4(a)]. Hence, for weak phason-strain-field magnitude, the induced magnitude variation of the 12 vectors of the 28–44 set is much weaker under a cubic  $\Gamma_4$  field, compared to a pentagonal  $\Gamma_5$  one: these vectors just “slide” on a sphere under  $\Gamma_4$ , while they move away from the sphere under  $\Gamma_5$ . A  $\Gamma_4$  phason-strain field will therefore cost less cohesive energy than a  $\Gamma_5$  one in the case of the Al-Li-Cu icosahedral phase.

We can apply similar considerations to the 20–32 set vectors  $(2/4, 0/0, 0/0)$ ,  $(0/0, 2/4, 0/0)$ ,  $(0/0, 0/0, 2/4)$ ,  $\dots$ , that are parallel to the twofold axes and generating the triacontahedron of the Al-Fe-Cu PBZ, with  $(4/\sqrt{2}, 0/0, 0/0)$ ,  $(0/0, 4/\sqrt{2}, 0/0)$ ,  $(0/0, 0/0, 4/\sqrt{2})$ ,  $\dots$ , as perpendicular vectors  $\mathbf{K}_\perp$ . Using Eq. (10), we can check that an  $M_T$  field shifts all the 30 vectors. While an  $M_{D5}$  field has no effect on the ten vectors that are perpendicular to the preserved fivefold axis, that is just the fivefold axis of the resulting  $D_5$  structure [see Fig. 4(b)]. So in the case of Al-Fe-Cu, for weak phason-strain-field magnitude (small  $\alpha$ ), a pentagonal  $\Gamma_5$  phason-strain field costs less cohesive energy than a cubic  $\Gamma_4$  field, which causes stronger PBZ deformation.

The above consideration implies certain symmetry constraints on the phason-strain field development: it is easier for a cubic  $\Gamma_4$  phason-strain field to develop in the Al-Li-Cu icosahedral phase than a  $\Gamma_5$  pentagonal one, and *vice versa* for the Al-Fe-Cu icosahedral phase. This is in agreement with our discussion on experimental observations (see Sec. II): the phason-strain field in Al-Li-Cu is described by the  $\Gamma_4$  representation, while Al-Fe-Cu can contain a  $\Gamma_5$  phason-strain field related to a pentagonal subgroup structure.

Finally, this mechanism explains the electronic specific-heat observations: the vectors with strong  $V_{\mathbf{K}}$  are hardly sensitive to phason strains, and the weaker  $V_{\mathbf{K}}$  vectors are shifted in such a way as to remain close to the Fermi surface. Therefore, the electronic DOS at the Fermi level remains almost the same in the Al-Li-Cu and Al-Fe-Cu icosahedral phases, in spite of the presence of the phason-strain fields.

## B. Vibrational

The situation for the vibrational term is totally different compared to that of the electronic one. The annealing re-

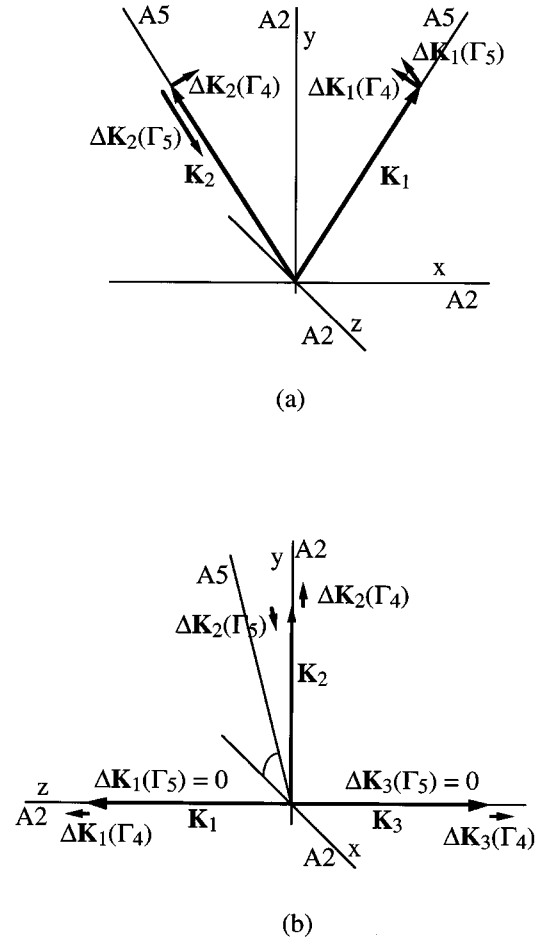


FIG. 4. Typical PBZ vector shifts  $\Delta\mathbf{K}$  under the phason-strain fields  $\Gamma_4$  ( $M_T$ ) and  $\Gamma_5$  ( $M_{D5}$ ): two vectors of the 28–44 set,  $\mathbf{K}_1 = (2/2, 2/4, 0/0)$ ,  $\mathbf{K}_2 = (\sqrt{2}/\sqrt{2}, 2/4, 0/0)$  (a), and three of the 20–32 set,  $\mathbf{K}_1 = (0/0, 0/0, 2/4)$ ,  $\mathbf{K}_2 = (0/0, 2/4, 0/0)$ , and  $\mathbf{K}_3 = (0/0, 0/0, \sqrt{2}/4)$  (b), are presented. The magnitudes of the phason-strain fields are taken for unity in the calculation of the module for all the  $\Delta\mathbf{K}$ . A2 and A5 indicate, respectively, the two- and fivefold symmetry axes. A5 in (b) represents also the fivefold axis of the  $D_5$  structure engendered by the  $\Gamma_5$  phason-strain field.

duces the vibrational contribution to the total specific heat by a factor of 2 for Al-Fe-Cu, while for Al-Li-Cu this contribution remains almost the same.

In order to better illustrate the vibrational density evolution through the phason-strain-field elimination for the Al-Fe-Cu samples, we replot their vibrational specific-heat  $C_{\text{vib}}$  data in a  $C_{\text{vib}}/T^3$  vs  $T^2$  diagram, this after the subtraction of the electronic contribution  $\gamma T$  (Fig. 5). In the Debye model,  $C_{\text{vib}}/T^3$  is proportional to  $D(\omega)/\omega^2$ , where  $D(\omega)$  is the phonon spectra and  $\omega$  is the corresponding mode frequency.<sup>27</sup> Thus this graph shows the vibrational density evolution with the sample structure states.

According to Fig. 5, for the Al-Fe-Cu samples, the low-energy vibrational DOS is enhanced in the phason-strained sample as compared to the annealed one. This enhancement is obviously associated with the phason-strain field, which is strongly eliminated through the annealing at 812 °C.

Low-energy mode density enhancements have also been observed by inelastic neutron scattering for Al-Fe-Cu QC samples of close chemical compositions. But these observa-

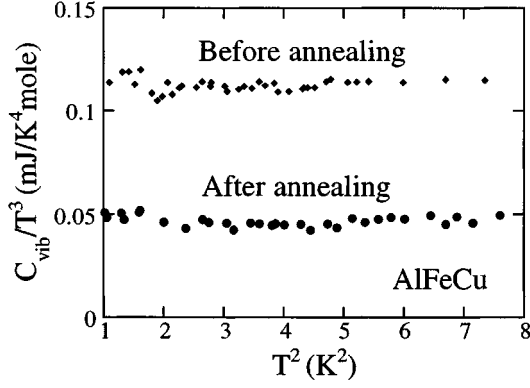


FIG. 5. The vibrational specific heat  $C_{\text{vib}}$  of icosahedral Al-Fe-Cu samples before ( $\blacklozenge$ ) and after ( $\bullet$ ) the 812 °C annealing treatment in a  $C_{\text{vib}}/T^3$  vs  $T^2$  diagram.

tions were made on as-cast samples,<sup>29</sup> which can contain various structural defaults as well as foreign phases.<sup>13</sup> Our observations, however, enable a direct comparison between monophased QC samples before and after the annealing treatment that allows phason-strain elimination. Moreover, the low-temperature specific-heat measurements explore a much lower energy range.

Figure 5 shows that the  $D(\omega)/\omega^2$  term for each sample remains constant in the measuring temperature range. This demonstrates well that the phonon dispersion follows a linear relation (the mode frequency varies linearly following the wave vector), and justifies the utilization of the Debye approximation. In the measuring temperature range, the  $D(\omega)$  enhancement cannot be attributed to the phason hopping, as the linear dispersion relation does not support resonance-mode contributions. Moreover, phason hopping is observed to occur at much higher temperature (above 600 °C).<sup>30</sup> In fact, as shown below, this anomaly can be attributed to a softening of the phonon shear modes. This implies a softening of the shear elastic modulus, in agreement with the group theory analysis (see Secs. II and III), and leads to a decrease of the Debye temperature.

The  $T=0$  Debye temperature can be related to the sound velocities by<sup>27</sup>

$$\theta_D(0) = \frac{h}{k_B} \left( \frac{3N}{4\pi V} \right)^{1/3} \bar{v}, \quad (11)$$

where  $\bar{v}$  is the mean sound velocity,  $N$  is the Avogadro number, and  $V$  is the molar volume. For an isotropic substance, we have  $\bar{v}^{-3} = (2v_T^{-3} + v_L^{-3})/3$ ,  $v_T$  and  $v_L$  being the transverse and longitudinal sound velocities.

The velocities  $v_T$  and  $v_L$  can be related to the shear and the bulk elastic moduli ( $\mu$  and  $B$ ) by<sup>31</sup>

$$v_T = \sqrt{\frac{\mu}{\rho}}, \quad v_L = \sqrt{\frac{B + \frac{4}{3}\mu}{\rho}}, \quad (12)$$

where  $\rho$  is the mass density. We can thus express the Debye temperature as a function of the two elastic moduli:

$$\theta_D(0) \propto \rho^{-1/6} [2\mu^{-3/2} + (B + \frac{4}{3}\mu)^{-3/2}]^{-1/3}. \quad (13)$$

The application of this isotropic model is justified by the large number of symmetry elements of the icosahedral structure.

For solids (even liquids), the elastic bulk modulus  $B$  is essentially related to the mean atomic volume. It is hardly sensitive to structure variations, if no strong atomic volume difference is involved. This is indeed the case for the two samples considered here, for which the lattice parameter is only changed by about 0.03% through annealing at 812 °C, according to the x-ray-diffraction experiments.<sup>13</sup> To illustrate this point, let us estimate the possible bulk modulus change due to parameter difference using Eq. (14), which is developed for intermetallic alloys:<sup>32</sup>

$$\frac{\Delta B}{B} = -\frac{\Delta a}{a} \frac{a'}{F(a')} \frac{dF(a')}{da'}, \quad (14)$$

where  $a$  is the mean interatomic distance and  $a'$  the interatomic distance related to structure variation. The function  $F(a')$  results from the Friedel oscillation, it has the asymptotic form  $\sim \sin(2k_F a')/a'^3$  with  $k_F$  the Fermi vector. Taking for  $\Delta a/a$  the value estimated from the x-ray-diffraction observation 0.03%, for  $a$  and  $a'$  the mean interatomic distance (of the order of 3 Å for metals) and for  $k_F$  the free-electron value  $k_{F, \text{free}} \approx 1.56 \text{ \AA}^{-1}$ , we estimate, using Eq. (14), that the relative change of the bulk modulus  $\Delta B/B$  is below 1%. Obviously, this is too weak to account for the Debye temperature difference between these two Al-Fe-Cu samples.

Hence, the  $\theta_{D0}$  decrease in the phason-strained sample should be attributed to the decrease of the elastic shear modulus  $\mu$ . This implies a softening of the phonon shear modes. Indeed, by neglecting the mass density variation, we can relate the change of the Debye temperature directly to that of the shear modulus using Eq. (13):  $\Delta\theta_{D0}/\theta_{D0} \approx \Delta\mu/2\mu$ . This relation enables us to estimate an elastic shear modulus difference of about 40%, between the phason-strained sample and the 812 °C annealed one. This result can be compared with Jaric and Mohanty's calculation, according to which phason strains reduce elastic shear modulus in icosahedral QC's. They also proposed that phason strains can be related to a martensitic instability,<sup>33</sup> which implies phonon shear mode softening.

For the Al-Li-Cu samples, the vibrational contribution remains the same before and after the annealing treatment. The corresponding Debye temperature, which is found, in both cases, to have a value of  $465 \pm 5$  K, is thus insensitive to the phason-strain elimination. We can also notice that this Debye temperature value can be compared to that obtained in experiments other than specific-heat measurements, such as ultrasound velocity characterization.<sup>34</sup> This observation indicates that the phason-strain field has no significant influence on the vibrational properties of the Al-Li-Cu quasilattice, contrary to the Al-Fe-Cu case.

The above observations can be well explained by the group theory analysis presented in Sec. III B: for icosahedral QC's there is no phason-phonon coupling for the  $\Gamma_4$  phason-strain field, while the  $\Gamma_5$  phason-strain field can be coupled to phonon shear modes. As we have mentioned in Sec. II, the phason-strain field in the Al-Li-Cu samples before annealing is essentially of  $\Gamma_4$  character, it has therefore no influence on

vibrational properties. In the Al-Fe-Cu case, various observations suggest that its phason-strain field has  $\Gamma_5$  character. The  $\Gamma_5$  phason-strain field is coupled to the  $\Gamma_5$  phonon shear mode, so the Debye temperature, as well as the elastic properties, are strongly affected by the phason strains.

### C. Remarks

Phason strains are likely to develop in QC samples during the growth process, thus the phason-strain-field symmetry should be related to the growth direction, i.e., to the growth morphology. The Al-Li-Cu QC phase grows in the form of triacontahedron, the presence of  $\Gamma_4$  strain fields in Al-Li-Cu can be related to the twofold axis growth direction. During the growth process, anisotropic phason-strain fields may develop preferentially along twofold axes, leading to corresponding distortions in the icosahedral structure, which are described by  $\Gamma_4$  representation. The Al-Fe-Cu QC phase grows as dodecahedron, and the phason-strain field in Al-Fe-Cu can also be related to the growth direction. For example, the development of a phason field along a fivefold axis can lead to a  $\Gamma_5$  phason-strain field.

Also, as shown by the above analysis, the Hume-Rothery stabilization mechanism in QC's implies that the phason-strain field should affect as little as possible the PBZ vectors, especially those of weaker intensity. This will induce certain constraints to the phason-strain-field symmetry, imposed by the electronic structure. It is interesting to notice that the preferential growth directions of the two alloys studied here correspond to the directions in which the development of a

phason-strain field affects less the PBZ. This may indicate some relationship between the electronic structure and the growth mode.

### VI. CONCLUSION

The results of low-temperature specific heat, measured on Al-Li-Cu and Al-Fe-Cu quasicrystalline samples before and after phason-strain-field elimination through annealing, are analyzed. The electronic specific heat for both Al-Li-Cu and Al-Fe-Cu is observed to be scarcely sensitive to the annealing treatments, this can be explained within the Hume-Rothery stabilization framework: the phason-strain-field symmetry is related to the pseudo-Brillouin-zone morphology, a phason-strain field should modify as little as possible the electronic cohesive energy, and consequently, leads to the weakest alteration of the pseudogap at the Fermi level. The phason-strain fields that are likely to be present in these systems ( $\Gamma_4$  for Al-Li-Cu and  $\Gamma_5$  for Al-Fe-Cu) satisfy such a condition. The annealing treatments have no influence on the vibrational specific heat of the Al-Li-Cu samples, but strongly decrease that of the Al-Fe-Cu ones. This can also be related to the phason-strain-field symmetry: a  $\Gamma_4$  phason-strain field is not coupled to any of the phonon fields, while a  $\Gamma_5$  one can be coupled to the  $\Gamma_5$  phonon field.

### ACKNOWLEDGMENTS

We thank Dr. P. Donnadiu and Dr. Y. Calvayrac for electron and x-ray-diffraction analyses of the samples, and Dr. M. Kléman for fruitful discussions.

- 
- <sup>1</sup>P. Bak, Phys. Rev. Lett. **54**, 1517 (1985); D. Levine, T. C. Lubensky, S. Ostlund, S. Ramaswamy, P. J. Steinhardt, and J. Toner, Phys. Rev. Lett. **54**, 1520 (1985).
- <sup>2</sup>P. A. Kalugin, A. Y. Ktaye, and L. S. Levitov, J. Phys. (Paris) Lett. **46**, L601 (1985).
- <sup>3</sup>M. Kléman and A. Pavlovitch, J. Phys. (Paris) Colloq. **47**, C3-229 (1986).
- <sup>4</sup>P. Bak, Phys. Rev. B **32**, 5764 (1985).
- <sup>5</sup>T. C. Lubensky, S. Ramaswamy, and J. Toner, Phys. Rev. Lett. **32**, 7444 (1985).
- <sup>6</sup>Y. Ishii, Phys. Rev. B **39**, 11 862 (1989).
- <sup>7</sup>O. Biham, D. Mukamel, and S. Strinkman, in *Introduction to Quasicrystals*, edited by M. V. Jaric (Academic, New York, 1988), p. 171.
- <sup>8</sup>T. C. Lubensky, J. E. S. Socolar, P. J. Steinhardt, P. A. Bancel, and P. A. Heiney, Phys. Rev. Lett. **57**, 1440 (1986).
- <sup>9</sup>M. Kléman, in *Quasicrystalline Materials*, edited by Ch. Janot and J. M. Dubois (World Scientific, Singapore, 1988), p. 318.
- <sup>10</sup>W. Hume-Rothery, J. Inst. Met. **295**, 35 (1926); J. Friedel and F. Dénoyer, C. R. Acad. Sci. **305**, 171 (1987).
- <sup>11</sup>K. Wang, C. Scheidt, P. Garoche, Y. Calvayrac, J. Phys. (France) I **2**, 1553 (1992); K. Wang, C. Degand, P. Donnadiu, P. Garoche, J. Non-Cryst. Solids **170**, 51 (1994); K. Wang, P. Donnadiu, and P. Garoche, in *Quasicrystals*, edited by Ch. Janot and R. Mosseri (World Scientific, Singapore, 1996), p. 351.
- <sup>12</sup>P. A. Heiney, P. A. Bancel, P. M. Horn, J. L. Jordan, S. LaPlaca, J. Angilello, and F. W. Gayle, Science **238**, 660 (1987).
- <sup>13</sup>Y. Calvayrac, A. Quivy, M. Bessière, S. Lefevre, M. Cornier-Quiquandon and D. Gratias, J. Phys. (Paris) **51**, 417 (1990); M. Bessière, A. Quivy, S. Lefevre, J. Devaud-Rzepski, and Y. Calvayrac, J. Phys. (France) I **1**, 1823 (1991).
- <sup>14</sup>P. Sainfort and B. Dubost, J. Phys. (Paris) Colloq. **47**, C3-321 (1986).
- <sup>15</sup>N. Yu, R. Portier, K. Yu-Zhang, and J. Bigot, Philos. Mag. Lett. **57**, 35 (1988).
- <sup>16</sup>Z. H. Mai, S. Z. Tao, L. Z. Zeng, and B. S. Zhang, Phys. Rev. B **38**, 12 913 (1988).
- <sup>17</sup>F. H. Li, G. Z. Pan, S. Z. Tao, M. J. Hui, Z. H. Mai, X. S. Chen, and L. Y. Cai, Philos. Mag. B **59**, 535 (1989).
- <sup>18</sup>P. Donnadiu and C. Degand, Philos. Mag. B **68**, 317 (1993).
- <sup>19</sup>D. Gratias, Y. Calvayrac, J. Devaud-Rzepski, F. Faudot, M. Harmelin, A. Quivy, and P. A. Bancel, J. Non-Cryst. Solids **153&154**, 482 (1993); M. Audier, Y. Bréchet, M. de Boissieu, and P. Guyot, Philos. Mag. B **63**, 1375 (1991).
- <sup>20</sup>N. Menguy, M. Audier, M. de Boissieu, P. Guyot, M. Boudard, and C. Janot, Philos. Mag. Lett. **67**, 35 (1993).
- <sup>21</sup>B. Dubost, J. M. Lang, M. Tanaka, P. Sainfort, and M. Audier, Nature (London) **324**, 48 (1986); B. Dubost, C. Colinet, and I. Ansara, in *Quasicrystalline Materials* (Ref. 9), p. 39.
- <sup>22</sup>K. Wang, P. Garoche, and Y. Calvayrac, in *Quasicrystalline Materials* (Ref. 9), p. 372.
- <sup>23</sup>C. Degand, K. Wang, and P. Garoche, J. Non-Cryst. Solids **153&154**, 478 (1993); P. Donnadiu, K. Wang, C. Degand, and P. Garoche, *ibid.* **183**, 100 (1995).

- <sup>24</sup>J. L. Wagner, B. D. Biggs, K. M. Wong, and S. J. Poon, Phys. Rev. B **38**, 7436 (1988).
- <sup>25</sup>B. D. Biggs, Y. Li, and S. J. Poon, Phys. Rev. B **43**, 8747 (1991).
- <sup>26</sup>T. Klein, C. Berger, D. Mayou, and F. Cyrot-Lackman, Phys. Rev. Lett. **66**, 2907 (1991).
- <sup>27</sup>C. Kittel, *Introduction to Solid State Physics*, 3rd ed. (Wiley, New York, 1966).
- <sup>28</sup>J. W. Cahn, D. Shechtman, and D. Gratias, J. Mater. Res. **1**, 13 (1986).
- <sup>29</sup>J. B. Suk, Mater. Sci. Eng. A **133**, 40 (1991).
- <sup>30</sup>S. Lyonnard, G. Coddens, R. Bellissent, Y. Calvayrac, and F. Fabi, in *Quasicrystals* (Ref. 11), p. 367.
- <sup>31</sup>R. N. Thurston, in *Physical Acoustics*, edited by W. P. Mason (Academic, New York, 1964), Vol. 1, Part A, p. 1.
- <sup>32</sup>A. Blandin, in *Alloys Behaviour and Concentrated Solid Solutions*, edited by T. B. Massalski (Gordon and Breach, New York, 1965), p. 50.
- <sup>33</sup>M. V. Jaric and U. Mohanty, Phys. Rev. B **38**, 9434 (1988); Phys. Rev. Lett. **58**, 230 (1987).
- <sup>34</sup>Gillian A. M. Reynolds, B. Golding, A. R. Kortan, and J. M. Parsey, Jr., Phys. Rev. B **41**, 1194 (1990).